Supplementary Material: Interplay of nanointerface curvature and calcium binding in weak polyelectrolytes coated nanoparticles

Rikkert J. Nap[a], Estefania Gonzalez Solveyra,[a], and Igal Szleifer[a*]
[a]*Department of Biomedical Engineering, Department of Chemistry, and Chemistry of Life Processes Institute,*
Northwestern University,
2145 Sheridan Road, Evanston, Illinois, 60208-3100, United States,

February 26, 2018

The following presentation is based and follows closely the presentation of the supporting material of Ref.[1]. Here, we present the total Helmholtz free energy describing an end-tethered weak polyelectrolyte layer in multivalent ions solutions and provide some numerical details. Further details can be found in Ref.[1] and its supporting information.

1 Free Energy Functional

The total Helmholtz free energy contains the following contributions

$$F = -TS_{\mathrm{conf}} - TS_{mix} + E_{elect} + E_{vdW} + F_{chem}. \tag{S1}$$

The conformational entropy of the polymers per unit area of the nanoparticle is given by

$$-\frac{S_{conf}}{k_B A(R)} = \sigma_p \sum_{\alpha} P(\alpha) \ln P(\alpha). \tag{S2}$$

Here, $P(\alpha)$ is the probability of finding a tethered polymer chain in conformation α. A polymer conformation is given by a set of the positions of all monomers of the polymer chain. The probability distribution function or pdf is the central quantity in the molecular theory, since any thermodynamic and structural properties of the polymers can be calculated from the probability distribution function. For instance, the average number density of the polymers at position r is given by

$$\langle \rho_p(r) \rangle = \frac{\sigma_p}{G(r)} \sum_{\alpha} P(\alpha) n(\alpha;r). \tag{S3}$$

Here $n(\alpha;r)\mathrm{d}r$ is the number of polymer segments that a polymer chain in conformation α has within volume element $[r, r+dr]$. The variable $n(\alpha;r)$ is input and depends on the molecular architecture and chemistry of the polymer. The variable r is the radial coordinate in either cylindrical or spherical coordinates. We employed cylindrical and spherical coordinates to reflect the symmetry of the cylindrical and spherical nanoparticle, and assumed the system to be laterally homogeneous and only explicitly anisotropic in the radial direction r Mathematically, the function $G(r) = A(r)/A(R)$ corresponds to the Jacobian determinant divided by the area of the cylindrical or spherical nanoparticle. Physically, $G(r)dr$ describes the change in volume as function of the distance away from the nanoparticle.[2] In cylindrical coordinates it equals (r/R) while for spherical coordinates it equals $(r/R)^2$, respectively.[3]

The second term in the free energy corresponds to the mixing or translational entropy of all mobile species

$$-\frac{S_{mix}}{k_B A(R)} = \sum_k \int \mathrm{d}r G(r) \rho_k(r) (\ln \rho_k(r) v_w - 1). \tag{S4}$$

The index k runs over all the different types of mobile species: the water molecule, the cations (Na^+ and Ca^{2+}), anion (Cl^-), proton (H^+), hydroxyl ion (OH^-), and the ion pair NaCl. The variable $\rho_k(r)$ is the number density of mobile species k and v_w is the volume of a water molecule. Note that the polymer-tethered NP is in contact with an aqueous solution of given pH containing monovalent NaCl and divalent $CaCl_2$ salt. For physiological concentrations we can assume that NaCl and $CaCl_2$ salt in the electrolyte solution are completely dissociated. For higher NaCl concentrations, also to be considered, not all NaCl's are completely dissociated in the aqueous solution and the possibility to form ion pairs, $Na^+ + Cl^- \rightleftharpoons NaCl$, has to be taken into account.[4] Hence, the ion pair is included as a separate chemical moiety in the mixing entropy.

The third term in the free energy functional describes the electrostatic contribution to the free energy[5] and is given by

$$\frac{\beta F_{elect}}{A(R)} = \beta \int \mathrm{d}r G(r) \left[\langle \rho_q(r) \rangle \psi(r) + \frac{1}{2} \varepsilon_0 \varepsilon_w \left(\nabla_r \psi(r) \right)^2 \right] + \beta \sigma_q \psi(R). \tag{S5}$$

Here $\psi(r)$ is the electrostatic potential, $\langle \rho_q(r) \rangle$ corresponds to the total charge density, and total σ_q corresponds to the surface charge density on the NP surface. In above functional ε_0 and ε_w correspond to the dielectric permittivity of vacuum and the relative dielectric

---

[*] corresponding author: email: igalsz@northwestern.edu

constant of the aqueous solution respectively, the latter one having a value of $\varepsilon_w = 78.5$. The total charge density is the sum of the charge number density of all charged species:

$$\langle \rho_q(r) \rangle = -e\langle \rho_p(r) \rangle \left(f_{A^-}(r) - f_{ACa^+}(r) \right) + \sum_{\substack{i \in \{Na^+, Ca^{2+}, \\ Cl^-, H^+, OH^-\}}} e z_i \rho_i(r). \tag{S6}$$

Here, the summation runs over all charged mobile species, with z_i corresponding to their valency. e is the unit of charge. The first part of the charge density describes the charge arising from the deprotonated monomers and the monomers that are condensed with one Ca^{2+} ion. Here $f_{A^-}(r)$ corresponds to the fraction of deprotonated polyacid monomers at position r, and $f_{ACa^+}(r)$ is the fraction of polyacid monomers that is bound with one calcium ion.

The fourth term in the free energy,F_{chem}, describes the free energy contribution arising from the acid-base equilibrium and condensation reactions. it is convenient to introduce the following polymer state fractions that are related to the different chemical states a monomer can be found in: namely, $f_{A^-}(r)$, $f_{AH}(r)$, $f_{ANa}(r)$, $f_{ACa^+}(r)$, and $f_{A_2Ca}(r)$. They correspond respectively to the fraction of monomers that are deprotonated, protonated, bound with one Na^+, bound with one Ca^{2+}, and the fraction of monomers found in an A_2Ca complex. With the definition of the monomer state fractions we can derive the chemical free energy associated with the chemical equilibria of the polymer acid monomers as given by in the main text. This chemical free energy is given by

$$\begin{aligned} \frac{\beta F_{chem}}{A(R)} = & \int \mathrm{d}r G(r) \langle \rho_p(r) \rangle \Big[f_{A^-}(r) \ln f_{A^-}(r) + f_{AH}(r) \ln f_{AH}(r) + f_{ANa}(r) \ln f_{ANa}(r) + f_{ACa^+}(r) \ln f_{ACa^+}(r) + \frac{f_{A_2Ca}(r)}{2} \ln \frac{f_{A_2Ca}(r)}{2} \\ & - \frac{1}{2} f_{A_2Ca}(r) \left(\ln \langle \rho_p(r) \rangle v_w - 1 \right) + f_{A^-}(r) \beta \mu^{\ominus}_{A^-} + f_{AH}(r) \beta \mu^{\ominus}_{AH} + f_{ANa}(r) \beta \mu^{\ominus}_{ANa} + f_{ACa}(r) \beta \mu^{\ominus}_{ACa} + \frac{1}{2} f_{A_2Ca}(r) \beta \mu^{\ominus}_{A_2Ca} \Big] \\ & + \sum_{k \in \{Na^+, Ca^{2+}, Cl^-, NaCl, H^+, OH^-\}} \beta \mu^{\ominus}_k \int \mathrm{d}r G(r) \rho_k(r). \end{aligned} \tag{S7}$$

The first six terms are related to the mixing entropy associated with the formation of the five different monomer states. Here, the first four terms correspond to the mixing entropy of the deprotonated, protonated, Na^+ condensed, and Ca^{2+} condensed state of the monomer. The fifth and sixth term correspond to entropic contribution associated with the A_2Ca complex. Here, we would like to draw attention to the factor 1/2 in the fifth term. The half occurs because one complex consists of two acidic monomers and one calcium ion. Hence, the total number density of complexes is half of the density of complexed acidic monomers. The sixth term corresponds to a loss of entropy that arises due to the reduction in the maximum number of possible states when two acidic monomers get combined into one A2Ca complex. The term appears for two-to-one and higher order complexation reactions. I t does not occur for one-to-one condensation. The next five terms of Eq. (reffechem) describe the enthalpic cost associated with the five states in which the monomers are found. Here, μ_γ corresponds to the standard free energy of forming a monomer in state i. The derivation of these terms is presented in further detail in the supporting material of Ref.[1]. The last contribution to F_{chem} describes the free energy associated with the standard chemical potential of Na^+, Ca^{2+}, Cl^- , NaCl, H^+, and OH^-. They are related to the dissociation reaction of NaCl and the auto-dissociation of water. Also included are the self-ionization of water and the ion pairing of NaCl. This chemical free energy is given by

In the main text we introduced above polymer state fractions, $f_{A^-}(r)$ and $f_{ACa^+}(r)$, as well as the other polymer state fractions associated with the different chemical states the monomer can be found in. Observe that the total number of monomers is conserved. Thus, the sum over all polymer state fractions at every position adds up to one, i.e.,

$$f_{A^-}(r) + f_{AH}(r) + f_{ANa}(r) + f_{ACa^+}(r) + f_{A_2Ca}(r) = 1. \tag{S8}$$

The repulsive interactions in the theory are modeled as excluded volume interactions. The intra chain interactions are considered exactly during generation of the polymer conformation. The intermolecular excluded volume interactions are accounted for by assuming that the system is incompressible at every position

$$\langle \phi_p(r) \rangle + \phi_w(r) + \sum_{\substack{k \in \{Na^+, Ca^{2+}, Cl^-, \\ NaCl, H^+, OH^-\}}} \phi_k(r) = 1. \tag{S9}$$

These volume constraints are enforced through the introduction of the Lagrange multipliers $\pi(r)$. The variable $\langle \phi_p(r) \rangle$ denotes the polymer volume fraction that is expressed as the polymer density times the sum over the different monomer states weighted with the volume of those states

$$\langle \phi_p(r) \rangle = \langle \rho_p(r) \rangle \left(f_{A^-}(r) v_{A^-} + f_{AH}(r) v_{AH} + f_{ANa}(r) v_{ANa} + f_{ACa^+}(r) v_{ACa} + \frac{1}{2} f_{A_2Ca}(r) v_{A_2Ca} \right). \tag{S10}$$

Here v_{A^-}, v_{AH}, v_{ANa}, and v_{ACa} correspond to the volume of the deprotonated acid monomer (A^-), protonated monomer (AH), sodium and calcium condensed monomer (ANa and ACa^+) respectively. v_{A_2Ca} is the volume of the A_2Ca complex. Because every complex consists of two acid monomers and one calcium ion, the density of the complexes at location r is $f_{A_2Ca}(r) \langle \rho_p(r) \rangle / 2$. Hence, the factor 1/2 appears in the last term of the polymer volume fraction. The volume fraction of the small mobile species is given by $\phi_k(r) = \rho_k(r) v_k$, where v_k is the volume of species k.

Finally, the E_{vdW} represents the non-electrostatic van der Waals interactions and is defined by

$$\frac{\beta E_{vdW}}{A(R)} = -\frac{\beta}{2}\int \mathrm{d}r \int \mathrm{d}r' A(R)G(r)G(r')\langle\rho_p(r)\rangle\chi(r,r')\langle\rho_p(r')\rangle, \tag{S11}$$

where $\chi(r,r')$ is an attractive van der Waals potential between a segment located at r and segment at r'. This term describes the effects of solvent quality. Here we assume good solvent conditions: $\chi(r,r') = 0$.

The free energy is minimized with respect to $P(\alpha)$, $\rho_i(r)$, and $f_k(r)$, and varied with respect to the electrostatic potential, $\psi(r)$, under the constraints of incompressibility and the fact that the system is in contact with a bath of cations, anions, protons, and hydroxyl ions. Therefore the proper thermodynamic potential is the semi-grand potential[2,6,7], which is given by

$$\begin{aligned}\frac{\beta W}{A(R)} \quad = \quad & \frac{\beta F}{A(R)} - \sum_{k\in\{w,NaCl,Cl^-,OH^-\}} \beta\mu_k \int \mathrm{d}r G(r)\rho_k(r) - \beta\mu_{H^+}\int \mathrm{d}r G(r)\left(\rho_{H^+}(r) + f_{AH}(r)\langle\rho_p(r)\rangle\right) \\ & -\beta\mu_{Na^+}\int \mathrm{d}r G(r)\left(\rho_{Na^+}(r) + f_{ANa}(r)\langle\rho_p(r)\rangle\right) - \beta\mu_{Ca^{2+}}\int \mathrm{d}r G(r)\left[\rho_{Ca^{2+}}(r) + \left(f_{ACa^+}(r) + \frac{1}{2}f_{A_2Ca}(r)\right)\langle\rho_p(r)\rangle\right] \\ & +\beta\int \mathrm{d}r G(r)\lambda(r)\langle\rho_p(r)\rangle\left[\sum_i f_i(r) - 1\right] + \beta\int \mathrm{d}r G(r)\pi(r)\left[\langle\phi_p(r)\rangle + \sum_k \rho_k(r)v_k - 1\right].\end{aligned} \tag{S12}$$

Here, μ_γ is the chemical potential of molecules of type γ. The second integral accounts for the total number of protons in the system, which is the sum of the free protons and those that are in the protonated state of the acidic monomers. The third and fourth integral correspond to the total number of sodium and calcium ions. These terms also include contributions arising from the various condensed states. In the free energy, $\lambda(r)$ are the Lagrange multipliers that enforce the constraint that the sum of the fractions of the different monomeric states adds up to one for all positions.

Minimization of the free energy yields the following expression for the local volume fraction of the solvent

$$\phi_w(r) = \rho_w(r)v_w = \exp\left(-\beta\pi(r)v_w\right), \tag{S13}$$

while the density of the ions reads

$$\rho_\gamma(r) = \frac{1}{v_w}\exp\left(\beta\mu_\gamma - \beta\mu_\gamma^{\ominus} - \beta\pi(r)v_\gamma - \beta\psi(r)z_\gamma e\right). \tag{S14}$$

It is important to point out that the chemical potential of water needs not be specified explicitly, because the incompressibility constraint reduces the number of thermodynamical independent variables. Therefore, the chemical potentials, μ_γ, are in reality exchange chemical potentials, which we define as the difference between the chemical potential of the species γ and that of water. Likewise the charge neutrality, the water self-dissociation equilibrium and the ion-ion paring of sodium with chloride ions reduce the number of thermodynamic independent variables further. The values of the exchange chemical potential of the remaining species can be expressed by relating them to their bulk concentrations: $\rho_\gamma^{bulk}v_w = \exp(\beta\mu_\gamma^{\ominus} - \beta\mu_\gamma - \beta\pi^{bulk}v_\gamma - \beta\psi_{bulk}z_\gamma)$, with $\psi_{bulk} = 0$, see below at Eq. S15. Further discussions of this aspect of the theory can be found in, e.g., Refs[2,7].

Functional variation of the free energy with respect to the electrostatic potential yields the Poisson equation and its boundary conditions

$$-\varepsilon_0\varepsilon_w\nabla_r^2\psi(r) = \langle\rho_q(r)\rangle; \quad -\varepsilon_0\varepsilon_w\left.\frac{d\psi(r)}{dr}\right|_{r=R} = \sigma_q; \quad \lim_{r\to\infty}\psi(r) = 0. \tag{S15}$$

Minimization with respect to the polymer state fractions and elimination of the Lagrange multiplier, $\lambda(r)$, results in following set of equations that govern the chemical equilibria

$$\frac{f_{A^-}(r)}{f_{AH}(r)} = K_{AH}^{\ominus}\frac{e^{-\beta\pi(r)\Delta v_{AH}}}{\rho_{H^+}(r)v_w}, \tag{S16}$$

$$\frac{f_{A^-}(r)}{f_{ANa}(r)} = K_{ANa}^{\ominus}\frac{e^{-\beta\pi(r)\Delta v_{ANa}}}{\rho_{Na^+}(r)v_w}, \tag{S17}$$

$$\frac{f_{A^-}(r)}{f_{ACa^+}(r)} = K_{ACa}^{\ominus}\frac{e^{-\beta\pi(r)\Delta v_{ACa}}}{\rho_{Ca^{2+}}(r)v_w}, \tag{S18}$$

$$\frac{f_{A^-}(r)^2\langle\rho_p(r)\rangle v_w}{\frac{1}{2}f_{A_2Ca}(r)} = K_{A_2Ca}^{\ominus}\frac{e^{-\beta\pi(r)\Delta v_{A_2Ca}}}{\rho_{Ca^{2+}}(r)v_w}. \tag{S19}$$

The variable $K_i^{\ominus} = \exp(-\beta\Delta G_i^{\ominus})$ corresponds to the chemical equilibrium and $\Delta G_i^{\ominus}$ is the standard free energy change. The chemical equilibrium constant $K_{AX}^{\ominus}$ is related to the experimental equilibrium constant $K_{AX} = C\exp(-\beta\Delta G_{AX}^{\ominus})$ of a single acidic monomer in infinitely dilute solution. Here C is a constant required for consistency of units and equal to $C = 1/N_Av_w$, where N_A is Avogadro's number. Here X corresponds to either AH, ANa, or ACa. For the reaction: $A_2Ca \rightleftharpoons 2A^- + Ca^{2+}$, the standard free energy change is given as $\Delta G_{A_2Ca}^{\ominus} = 2\mu_{A^-}^{\ominus} + \mu_{Ca^{2+}}^{\ominus} - \mu_{A_2Ca}^{\ominus}$, while the change in volume is equal to $\Delta v_{A_2Ca} = 2v_{A^-} + v_{Ca^{2+}} - v_{A_2Ca}$. Similar to the chemical equilibrium of AH, ANa, and ACa, the chemical constant $K_{A_2Ca}^{\ominus}$ can be related to the experimental equilibrium constant $K_{A_2Ca} = C'\exp(-\beta\Delta G_{A_2Ca}^{\ominus})$ of a single A_2Ca complex group in dilute solution. The constant C' is equal to $C' = 1/(N_Av_w)^2$. The constant C and C' can be obtained by re-expressing Eq. (S16) and Eq. (S19) in terms of the concentrations of the products and reactants

Table S1 Dissociation Constants and standard reaction binding free energy $\Delta G^{\ominus}$ for acrylic acid (AA) monomers.

reaction	$pK(AA)$	$\Delta G_b^{\ominus}(AA)$ (kJ/mol)
$\mathrm{AH} \rightleftharpoons \mathrm{A}^- + \mathrm{H}^+$	5.0	-38.5
$\mathrm{ANa} \rightleftharpoons \mathrm{A}^- + \mathrm{Na}^+$	-0.40	-7.5
$\mathrm{ACa}^+ \rightleftharpoons \mathrm{A}^- + \mathrm{Ca}^{2+}$	1.0	-15.7
$\mathrm{A_2Ca} \rightleftharpoons 2\mathrm{A}^- + \mathrm{Ca}^{2+}$	4.0	-42.7

The values for the acid-base equilibrium of the weak carboxylic acid acid is known experimentally.[8,9] However, the chemical equilibrium constants of the various ion condensation reactions are less well known. In particular the binding constant of the calcium carboxylic complex (A_2Ca) is difficult to obtain. Refs.[10,11] reported a value of $K_{A_2Ca} = 10^{-4.3}\,M^2$ and $10^{-5}\,M^2$ respectively. Refs.[12,13] reported similar values for slightly different monomers and ions. Because not all binding constants are experimentally readily available. We performed new molecular dynamics simulations to supplement the available data. Further details of the simulation methods can be obtained in the arXiv.org link arXiv:1801.05888 [physics.chem-ph]. (Ref.[14]) and the supporting information of[1]. The values of the dissociation equilibrium constants and the standard reaction free energies for the AH, ANa, ACa^+, and $\mathrm{A_2Ca}$ dissociable groups employed are listed in table S1. We chose a value of $K_{A_2Ca} = 10^{-4}$ based on the simulations result and available experimental data. Observe that the corresponding binding free energy equals $\Delta G_b^{\ominus}(A_2Ca) = -\Delta G^{\ominus}(A_2Ca) = -42.7\,\mathrm{kJ/mol}$ which is close to the experimental values of $\Delta G_b = -44.4\,\mathrm{kJ/mol}$ and $-48.4\,\mathrm{kJ/mol}$ of Refs.[10,11].

Minimization with respect to $P(\alpha)$ leads to

$$\begin{aligned} P(\alpha) &= \frac{1}{q}\exp\left(-\int \mathrm{d}r\, n(\alpha;r)\left(1+\beta\lambda(r)\right)\right) && \text{(S20)} \\ &= \frac{1}{q}\exp\left(-\int \mathrm{d}r\, n(\alpha;r)\left(\beta\pi(r)v_{A^-} + \beta\psi(r)z_{A^-}e + \ln f_{A^-}(r) + \beta\mu^{\ominus}_{A^-}\right)\right). && \text{(S21)} \end{aligned}$$

Here q is a normalization constant that ensures that $\sum_\alpha P(\alpha) = 1$. Here $\lambda(r)$ is a Lagrange multiplier that ensures that equation (S8) is satisfied: the fractions associated with the different chemical states for the monomers must add up to on one. In the second line we used one of five equivalent expression for $\lambda(r)$. Notice that the pdf explicitly depends on among the degree on deprotonation, which via Eq. S8 is directly related to the fraction of acid monomers that form calcium bridges, and ion pairs with sodium and calcium ions. For further details on is referred to the supporting material of Ref.[1].

The unknowns in Eq. (S13), Eq. (S14), and Eq. (S16) through Eq. (S19) are the Lagrange multipliers or lateral pressures, $\pi(r)$, the electrostatic potential, $\psi(r)$, and the degree of complexation, $f_{A_2Ca}(r)$. The degree of protonation of the acidic groups and the amount of condensation of sodium and calcium as well as the density of the ions, the solvent and polymers are known once the lateral pressures, the electrostatic potential, and degree of calcium complexation are known. Solutions of these variables can be obtained numerically. This is accomplished in the following way. Expressions of the volume fractions of all components are substituted into the incompressibility constraint, the Poisson equation, and the reaction equation Eq. (S19). This results in a set of non-linear integro differential equations whose solution will determine the lateral pressure, the electrostatic potential, and the degree of calcium complexation. By discretizing space, the differential equations are converted into a set of coupled non-linear algebraic equations that can be solved by standard numerical techniques.[15] Details on the discretization procedure and numerical methods can be found in Refs.[2] and the section "Numerical methodology". The inputs required to solve the non-linear equations are a set of polymer conformations, the pH, the salt concentrations of NaCl and $\mathrm{CaCl_2}$, the volume of all species, the surface density of the polymers end-tethered to the nanoparticle, the radius of the nanoparticle, the various dissociation equilibrium constants pK listed in table S1, and the dissociation constant of the NaCl ion pair.[4] Details on the chain model used to generate a set of conformations can be found in the section "Chain model".

2 Numerical methodology

Substituting the equations for the polymer, solvent and ion densities Eqs. (S3), (S13), and (S14) into the packing constraint, Eq.(S9), the generalized Poisson-Boltzmann equation, Eq. (S15), and the chemical reaction equations, Eqs. (S16), (S17), (S18), (S19), and (S8) results in a set of coupled integro-differential equations. The unknown of these equations are the position dependent lateral pressure, $\pi(r)$, electrostatic potential, $\psi(r)$, and fraction of calcium bridges, $f_{A_2Ca}(r)$. A numerical solution for the lateral pressure, $\pi(r)$, electrostatic potential, $\psi(r)$ and fraction of calcium bridges, $f_{A_2Ca}(r)$, is obtained by discretization of the packing constraints, Eq. (S9), and the generalized Poisson equation, Eq. (S15), and the reaction describing the formation of calcium bridges, Eq. (S19). The equations are discretized by dividing the r-coordinate into cylindrical spherical or shells of thickness δ. Position dependent functions are assumed to be constant within a cylindrical or spherical shell, hence integrations can be replaced by summations. The integral of a general position dependent function $f(r)$ then becomes:

$$\int_V \mathrm{d}r G(r) f(r) = \sum_i \int_{(i-1)\delta+R}^{i\delta+R} \mathrm{d}r\, G(r) f(r) \approx \delta \sum_i f(i)\Delta G(i), \tag{S22}$$

with

$$\Delta G(i) = \frac{1}{\delta}\int_{(i-1)\delta+R}^{i\delta+R} \mathrm{d}r\, G(r). \tag{S23}$$

Here $f(i)$ denotes the value which the function $f(r)$ attains within the cylindrical or spherical region located between $(i-1)\delta + R \leq r < i\delta + R$. Recall that $G(r) = A(r)/A(R)$ corresponds to the Jacobian determinant divided by the area of the nanoparticle. Hence $\Delta G(i)$ is the proportional to the volume of the discrete shell i.

The packing constraint, Eq. (S9), in discrete form for grid cell (i) reads

$$\langle \phi_p(i) \rangle + \phi_w(i) + \phi_{Na^+}(i) + \phi_{Cl^-}(i) + \phi_{NaCl}(i) + \phi_{H^+}(i) + \phi_{OH^-}(i) + \phi_{Ca^{2+}}(i) = 1. \tag{S24}$$

The volume fraction of water, Eq. (S13), the polymer density, Eq. (S3), and the pdf, Eq. (S20), in discrete form become

$$\begin{aligned}
\phi_w(i) &= \exp(-\beta\pi(i)v_w), && \text{(S25)}\\
\langle \rho_\gamma(i) \rangle &= \frac{\sigma}{\delta \Delta G(i)} \sum_\alpha P(\alpha) n(\alpha;i) && \text{(S26)}\\
n(\alpha;i) &\equiv \int_{(i-1)\delta+R}^{i\delta+R} \mathrm{d}r\, n(\alpha;r) && \text{(S27)}\\
P(\alpha) &= \frac{1}{q} \prod_i \exp\left[-n(\alpha;i)\left(\beta\pi(i)v_{A^-} + e\beta\psi(i) + \ln(f_{A^-}(i))\right]\right. . && \text{(S28)}
\end{aligned}$$

The volume fraction of the counterion, coions, protons, and hydroxyl ions, (Eq.(S14)), in discretized space are:

$$\begin{aligned}
\phi_{Na^+}(i) &= \phi_{Na^+,bulk} \exp(-\beta(\pi(i) - \pi_{bulk})v_{Na^+} - e\beta\psi(i)), && \text{(S29)}\\
\phi_{Cl^-}(i) &= \phi_{Cl^-,bulk} \exp(-\beta(\pi(i) - \pi_{bulk})v_{Cl^-} + e\beta\psi(i)), && \text{(S30)}\\
\phi_{H^+}(i) &= \phi_{H^+,bulk} \exp(-\beta(\pi(i) - \pi_{bulk})v_{H^+} - e\beta\psi(i)), && \text{(S31)}\\
\phi_{OH^-}(i) &= \phi_{OH^-,bulk} \exp(-\beta(\pi(i) - \pi_{bulk})v_{OH^-} + e\beta\psi(i)). && \text{(S32)}\\
\phi_{Ca^{2+}}(i) &= \phi_{Ca^{2+},bulk} \exp(-\beta(\pi(i) - \pi_{bulk})v_{Ca^{2+}} - 2e\beta\psi(i)). && \text{(S33)}\\
\phi_{NaCl}(i) &= \phi_{NaCl,bulk} \exp(-\beta(\pi(i) - \pi_{bulk})v_{NaCl}). && \text{(S34)}
\end{aligned}$$

The above volume fractions depend on the lateral pressure, electrostatic potential, and on the bulk volume fractions. The chemical potentials of the counter ions, co ions, protons, and hydroxyl ions are related to their bulk volume fractions.[2] These bulk values are input to the theory.

The chemical reaction Eqs. (S16), (S17), (S18), (S19) are in discrete form

$$\begin{aligned}
\frac{f_{A^-}(i)}{f_{AH}(i)} &= K^{\ominus}_{AH} \frac{e^{-\beta\pi(i)\Delta v_{AH}}}{\rho_{H^+}(i)v_w}, && \text{(S35)}\\
\frac{f_{A^-}(i)}{f_{ANa}(i)} &= K^{\ominus}_{ANa} \frac{e^{-\beta\pi(i)\Delta v_{ANa}}}{\rho_{Na^+}(i)v_w}, && \text{(S36)}\\
\frac{f_{A^-}(i)}{f_{ACa^+}(i)} &= K^{\ominus}_{ACa} \frac{e^{-\beta\pi(r)\Delta v_{A_2Ca}}}{\rho_{Ca^{2+}}(r)v_w}, && \text{(S37)}\\
\frac{[f_{A^-}(i)]^2 \langle \rho_A(i) \rangle v_w}{\frac{1}{2} f_{A_2Ca}(i)} &= K^{\ominus}_{A_2Ca} \frac{e^{-\beta\pi(i)\Delta v_{A_2Ca}}}{\rho_{Ca^{2+}}(i)v_w}, && \text{(S38)}\\
1 &= f_{A^-}(i) + f_{AH}(i) + f_{ANa}(i) + f_{ACa^+}(i) + f_{A_2Ca}(i). && \text{(S39)}
\end{aligned}$$

The discretized Poisson equation, in cylindrical coordinates, is

$$\left(1 + \frac{\delta}{r_i}\right)\psi(i+1) - 2\psi(i) + \left(1 - \frac{\delta}{r_i}\right)\psi(i-1) = -\varepsilon_w\varepsilon_0\delta^2\rho_q(i), \tag{S40}$$

here $r_i = (i - 1/2)\delta + R$ denotes the middle of the cylindrical grid cell (i) in the radial direction.

The discretized Poisson equation, in spherical coordinates, is

$$\left(1 + \frac{\delta}{2r_i}\right)\psi(i+1) - 2\psi(i) + \left(1 - \frac{\delta}{2r_i}\right)\psi(i-1) = -\varepsilon_w\varepsilon_0\delta^2\rho_q(i), \tag{S41}$$

here $r_i = (i - 1/2)\delta + R$ denotes the middle of the spherical grid cell (i) in the radial direction. The discretized electrostatic boundary condition for the both the cylindrical as well as spherical surface $(r = R)$ reads:

$$\psi(1) - \psi(r = R) = -\delta\varepsilon_w\varepsilon_0\sigma_q. \tag{S42}$$

Here $\psi(r = R)$ is the electrostatic potential at the nanoparticle surface.

Substituting Eqs. (S25), through (S34) into the constraint equation (S24), the Poisson Eq. (S40) for cylindrical surfaces or (S41) for spherical surfce , the electrostatic boundary condition (Eq. S42) and the chemical reaction equations Eqs. (S35) through (S39) result in a set of coupled nonlinear algebraic equations which can be solved by standard numerical methods.[15]

3 Chain model

We use the three-state rotational isomeric state (RIS) model of Flory[16] in order to generate a representative set of chain conformations. These conformations are generated by a simple sampling procedure that takes into account the self-avoidance of the polymer chain. Through appropriate translational and rotational adjustments, the generated chain conformations are end-tethered the surface of the NP of given radius. Internal self-avoidance of the chain and the chain with the NP core are enforced. One set of chain conformations is generated once for each sequence of copolymers and is used for all calculations reported in this paper. The number of conformations is $1 \cdot 10^6$. We used a discretization length $\delta = 0.5\,\mathrm{nm}$. Below in tables S2 and S3 we list the value of the volume of the monomers and ions used throughout the calculations. We use $\Delta v_{AH} = v_w$ for the acid base equilibrium and set $\Delta v_k = 0$ for all other reactions.

Table S2 Volume and segment length of AA monomers.

	AA
$\ell(nm)$	0.362
$v_p(nm^3)$	0.07448

Table S3 Volume and charge of ions.

	w	H^+	OH^-	Na^+	Cl^-	Ca^{2+}
$v(nm^3)$	0.03	0.03	0.03	0.0044	0.011	0.0050
$q(e)$	0	+1	-1	+1	-1	+2

4 Additional Results

In this section, we present additional results that support and supplement the discussion presented in the main text.

Fig. S1 shows the fraction of deprotonated monomers and the average total polymer charge per unit length in a end-tethered poly(acrylic acid) layer end-tehered to a cylindrical nanoparticle of radius R = 4.0 nm, as a function of pH for different calcium concentrations. The figure expands on the discussion of Fig. 3 in the main text. A detailed analysis of Fig. S1 goes beyond the scope of this work. We refer the interested reader to the thorough discussion provided for a spherical system in Ref.[1]

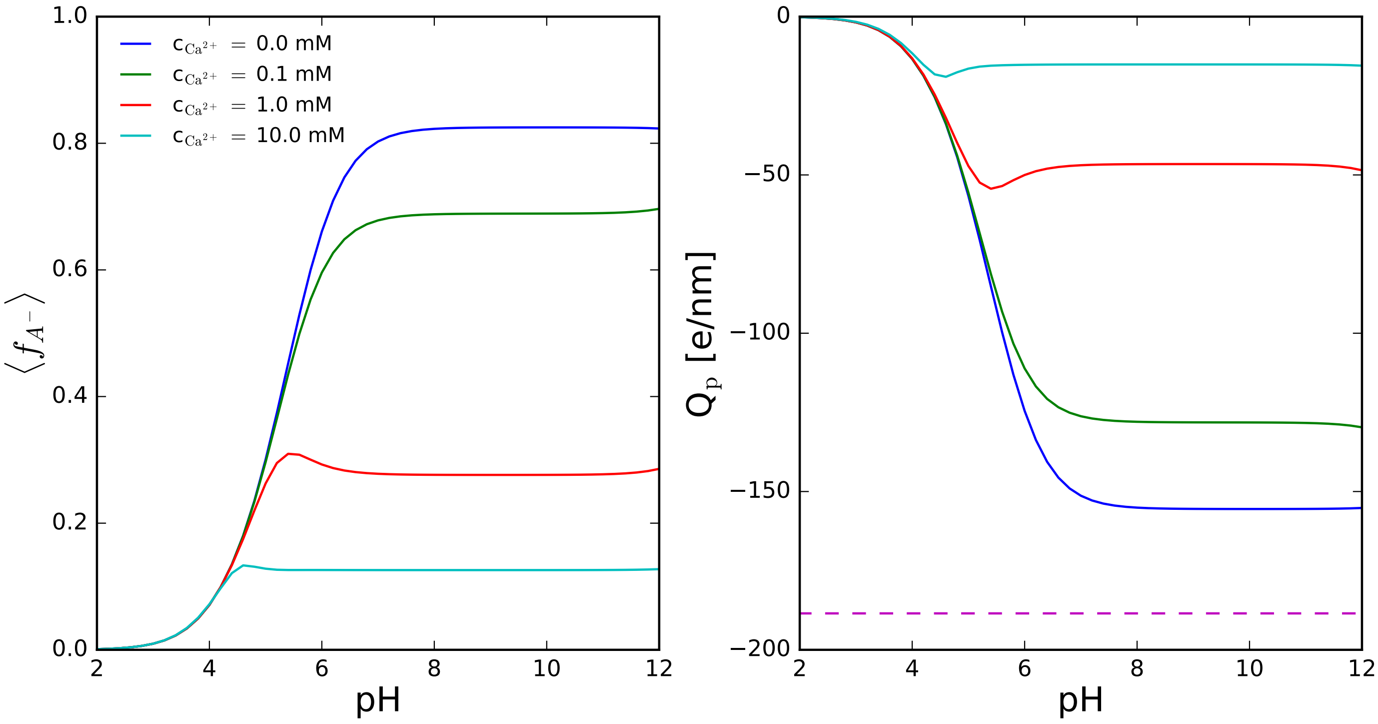

Figure S1 The fraction of acid monomers (left panel) in the end-tethered poly(acrylic acid) layer and average total polymer charge per unit length (right panel) as a function of the solution's pH for different amounts of Ca^{2+}, as indicated in the legend. The NaCl concentration is 150 mM. The radius, surface coverage, and molecular weight are equal to $R = 4\,\mathrm{nm}$, $\sigma = 0.15\,\mathrm{nm}^{-2}$, and n=50, respectively. The lower dashed line in the right panel correspond the the maximum feasible total polymer charge per unit length.

Fig. S2 shows the fraction of monomers forming a calcium bridge in an end-tethered poly(acrylic acid) layer as a function of the Ca^{2+} concentration. The figure directly complements the height vs Ca^{2+} concentration as shown in Fig. 3 in the main text.

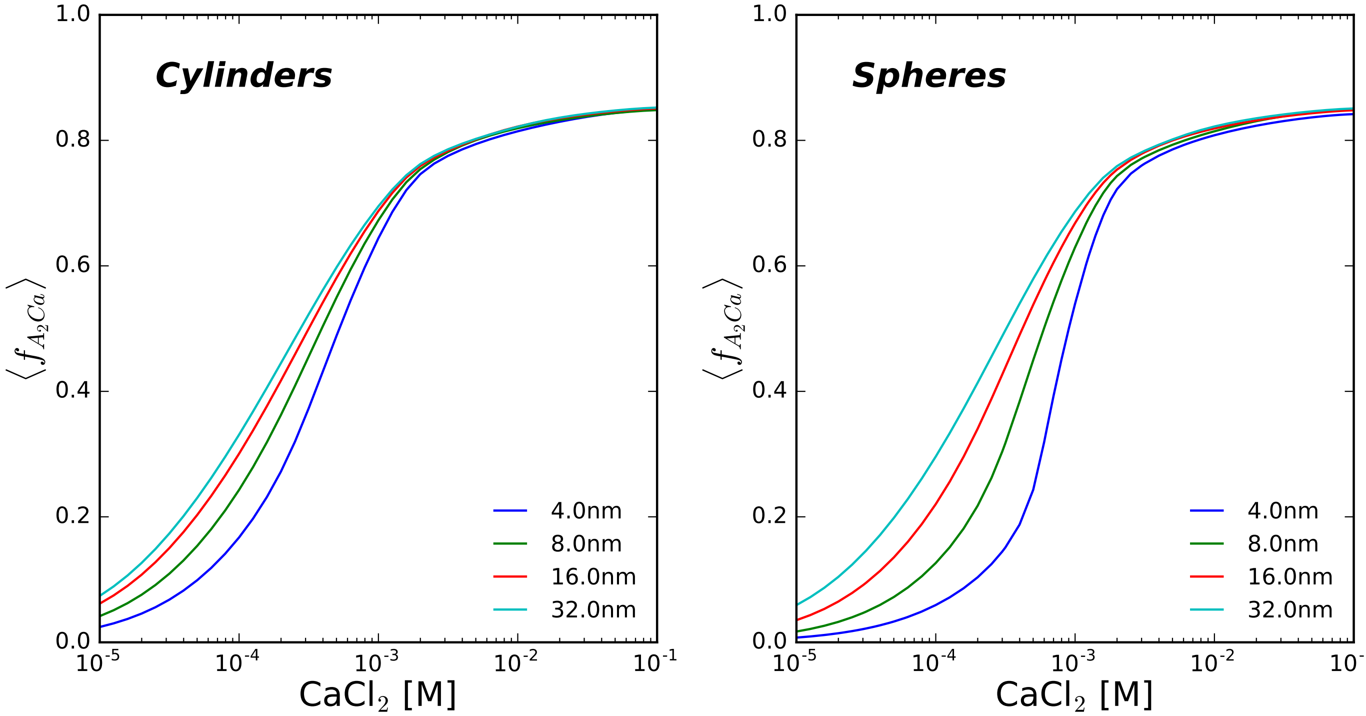

Figure S2 The fraction of monomers forming a calcium bridge in the end-tethered poly(acrylic acid) layer as a function of the Ca^{2+} concentration. The different lines correspond to increasing radii of the nanoparticle. The pH is equal to 7.4 and the NaCl concentration is 150 mM. The radius, surface coverage, and molecular weight are equal to $R = 4\,\text{nm}$, $\sigma = 0.15\,\text{nm}^{-2}$, and n=50, respectively.

Fig. S3 shows the polymer height of the end-tethered poly(acrylic acid) layer as a function of the surface density of the polymers for spherical and cylindrical nanoparticles. The figure directly complements the discussion in the last section of the main text (Fig. 6). At zero calcium concentration the height of polymer layer increases as functions of surface density. With increasing surface density, the polymers experience more excluded volume repulsions and the polymers stretch in order to reduce those interactions and the layer swells. For the low calcium concentration of $0.1\,\text{mM}$ the layer does not collapse upong increasing surface density. Instead we observe non-monotonic change in the height of the layer as function calcium concentration. With increasing surface density of the polymer layer first swells slightly before starting to contract slightly. First, due the increased excluded volume interaction the layer swells (similar to what occurs to zero added calcium). With increased monomer density, more calcium bridges occur leading to a contraction of the layer. However the calcium concentration is insufficient to form enough calcium bridges to effect a complete collapse and the layer remains in a swollen state. At a calcium concentration of $1\,\text{mM}$ the height of polymer layer of cylinder as well as sphere transitions from a swollen to a collapsed state. Increasing surface density leads to an increase in the polymer density. This facilitates the formation of more calcium bridges, causing the layer to collapse. The observed trend and its explanation is similar to the explanation for the height dependence on as function of curvature, as outlined in the main text. Finally, at a large calcium concentration of $10\,\text{mM}$ the excess amount of calcium leads to a high number of calcium bridges and all layers collapse. Note, the height of the collapsed state increases since the total amount of monomers increases.

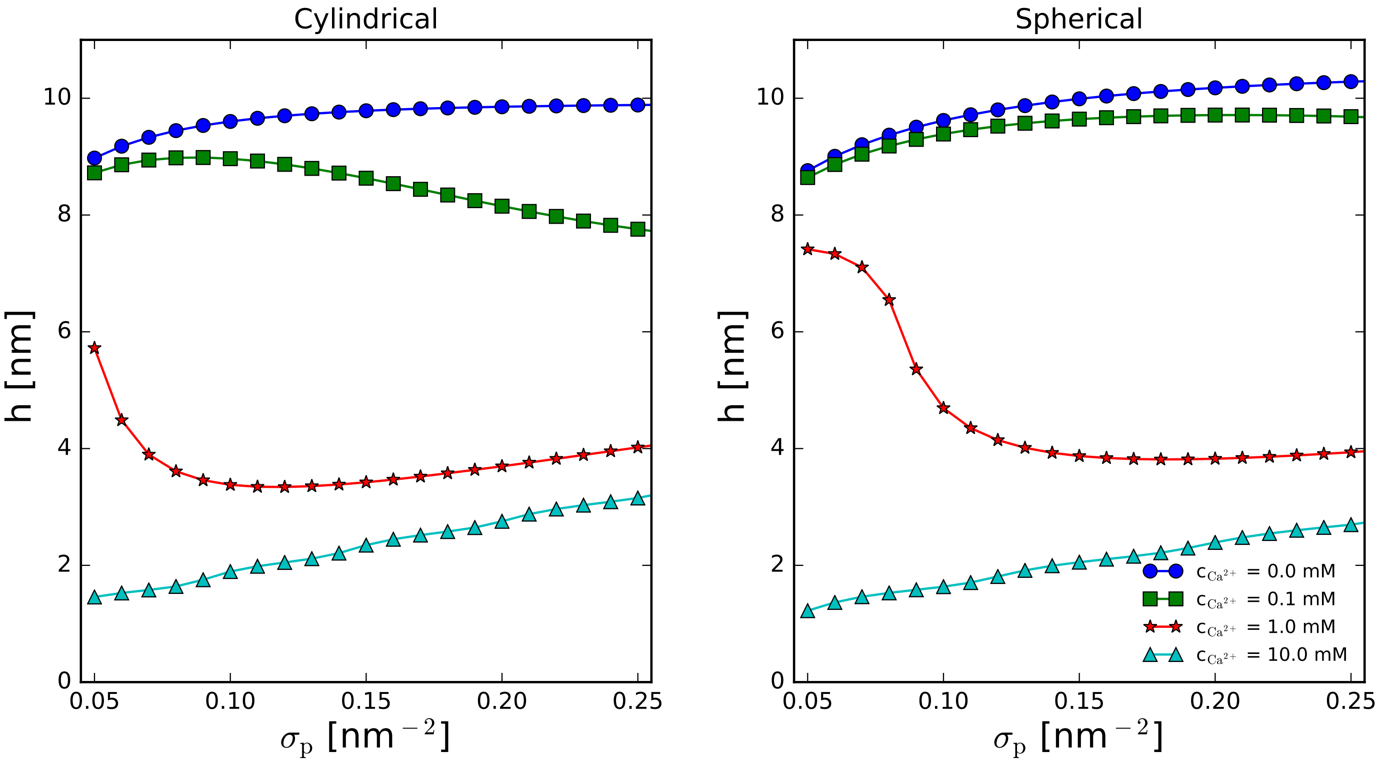

Figure S3 The height of a poly(acrylic acid) end-tethered layer as a function of polymer surface density for cylindrical (left panel) and spherical nanoparticles (right panel) of radius $R = 4\,\mathrm{nm}$. The different lines correspond to different Ca^{2+} concentrations, as indicated in the legend. The pH of the solution and the amount of NaCl correspond to physiological conditions, 7.4 and 150 mM respectively. The number of segments is 50.

References

[1] R. J. Nap, S. H. Park and I. Szleifer, *Soft Matter*, 2018, accepted for publication, doi: 10.1039/C7SM02434G.

[2] R. Nap, P. Gong and I. Szleifer, *J. Polym. Sci., Part B: Polym. Phys.*, 2006, **44**, 2638–2662.

[3] M. A. Carignano and I. Szleifer, *J. Chem. Phys.*, 1995, **102**, 8662–8669.

[4] R. J. Nap, S. H. Park and I. Szleifer, *J. Polym. Sci., Part B: Polym. Phys.*, 2014, **52**, 1689–1699.

[5] J. Schwinger, L. L. DeRaad, Jr., K. A. Milton and W.-Y. Tsai, *Classical Electrodynamics*, Persus Books, Reading Massachusetts, 1998.

[6] R. J. Nap, M. Tagliazucchi and I. Szleifer, *J. Chem. Phys.*, 2014, **140**, 024910.

[7] G. S. Longo, M. Olvera de la Cruz and I. Szleifer, *J. Chem. Phys.*, 2014, **141**, 124909.

[8] *CRC handbook of Chemistry and Physics*, ed. D. R. Lide, CRC Press, 84th edn, 2003.

[9] J. P. Guthrie, *Can. J. Chem.*, 1978, **56**, 2342–2354.

[10] T. Miyajima, M. Mori and S. Ishiguro, *J. Coll. Int. Sci.*, 1997, **187**, 259–266.

[11] C. G. Sinn, *PhD thesis*, Universität Potsdam, 2004.

[12] A. Ikegami and N. Imai, *J. Polym. Sci.*, 1962, **56**, 133–152.

[13] I. Pochard, P. Couchot and A. Foissy, *Colloid and Polym. Sci.*, 1998, **276**, 1088–1097.

[14] S. H. Park, R. J. Nap and I. Szleifer, *ArXiv e-prints*, 2018, arXiv:1801.05888[physics.chem–ph].

[15] A. C. Hindmarsh, P. N. Brown, K. E. Grant, S. L. Lee, R. Serban, D. E. Shumaker and C. S. Woodward, *ACM Trans Math Software*, 2005, **31**, 363–396.

[16] P. J. Flory, *Statistical Mechanics of Chain molecules*, Oxford University Press, New York, 1989.